

# Anomalous temperature dependence of the photoluminescence properties in GaAs triple quantum wells with growth islands

A Satake<sup>†</sup>, K Hayata<sup>†</sup>, N Shiraishi<sup>†</sup>, K Fujiwara<sup>†</sup>,  
L Schrottke<sup>‡</sup>, R Hey<sup>‡</sup>, and H T Grahn<sup>‡</sup>

<sup>†</sup> Kyushu Institute of Technology, Tobata, Kitakyushu 804-8550, Japan

<sup>‡</sup> Paul-Drude-Institut für Festkörperelektronik, Hausvogteiplatz 5-7, 10117 Berlin, Germany

**Abstract.** We have investigated the effect of different cladding layer configurations on the photoluminescence (PL) properties of GaAs triple quantum wells (QWs) with different well thicknesses ( $L_z=7.8, 5.5,$  and  $3.5$  nm) embedded in  $\text{Al}_{0.17}\text{Ga}_{0.83}\text{As}$  barriers. In sample 1, the cladding layers consist of ternary alloy  $\text{Al}_{0.3}\text{Ga}_{0.7}\text{As}$  layers, while in sample 2 they are formed by GaAs/AlAs short period superlattices. At low temperatures, the cw PL spectra for sample 1 show a non-uniform intensity distribution over the three QW excitonic lines. The PL intensity for the widest QW (7.8 nm) is much weaker than that for the other QWs. Furthermore, an anomalous temperature dependence of the PL transients of the widest QW is observed, which differs from the one expected for the excitonic radiative recombination lifetime. However, sample 2 exhibits the typical temperature dependence of the PL lifetime. The temperature dependence of the PL dynamics indicates that the non-uniform distribution of the PL intensity at low temperatures in the former sample is a result of a competition between carrier relaxation and capture processes.

## 1. Introduction

In quantum well (QW) structures with different well thicknesses separated by sufficiently thick barriers, the confined electron and hole states in each well are considered to be independent. Therefore, the relevant emission properties of each well should exhibit an independent characteristic without any correlation between the QWs. However, complex photoluminescence (PL) and PL excitation spectra have been reported in recent studies of electrically isolated QWs [1-3], suggesting that the QWs are by no means independent with respect to exciton formation (carrier relaxation and capture) and radiative recombination. In this contribution, the effect of different cladding layer configurations on the PL properties is studied in two samples containing

three GaAs QWs embedded in  $\text{Al}_{0.17}\text{Ga}_{0.83}\text{As}$  barriers using steady-state and time-resolved PL experiments as a function of lattice temperature ( $T$ ).

## 2. Experimental

The two samples were grown on GaAs (100) substrates by molecular-beam epitaxy. The sample structure is shown in Fig. 1(a). Each sample consists of a 600 nm GaAs buffer, the GaAs/ $\text{Al}_{0.17}\text{Ga}_{0.83}\text{As}$  triple QW structure embedded in the respective cladding layers, and a 3.5 nm GaAs cap layer. The triple QW structure contains three undoped GaAs QWs with different well widths of 7.8 (QW1), 5.5 (QW2), and 3.5 nm (QW3) starting from the substrate side. They are separated by 36 nm  $\text{Al}_{0.17}\text{Ga}_{0.83}\text{As}$  barriers and embedded in 72 nm  $\text{Al}_{0.17}\text{Ga}_{0.83}\text{As}$  barriers as shown in Fig. 1(b), which displays a potential diagram of the triple QW structure. The QW layers were prepared using 2-minutes growth interruption at the GaAs well interfaces under arsenic beam flux. The two samples differ only in their cladding layer configuration. That is, the cladding layers are composed of either an  $\text{Al}_{0.3}\text{Ga}_{0.7}\text{As}$  ternary alloy in sample 1 or a GaAs/AlAs (2.3 nm/1.0 nm) short-period superlattice in sample 2. The average Al mole fraction is the same for both cladding layers. Steady-state PL spectra were measured between 20

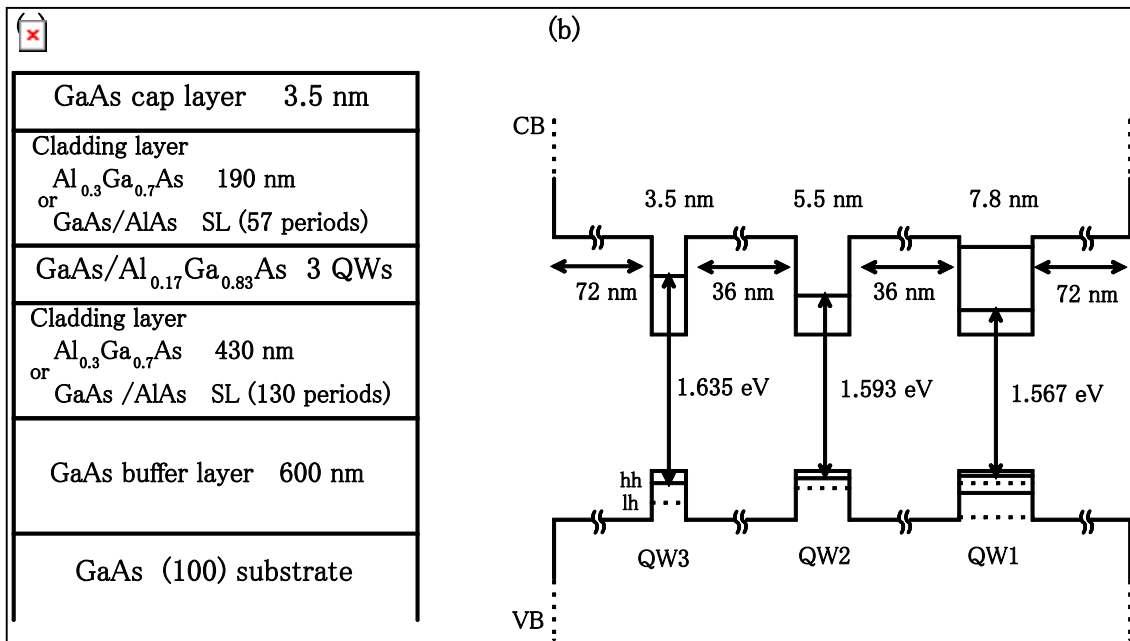


Fig.1 (a) Schematic diagram of the two investigated samples differing only in their cladding layer configuration, which are composed of either an  $\text{Al}_{0.3}\text{Ga}_{0.7}\text{As}$  ternary alloy (sample 1) or a GaAs/AlAs (2.3 nm/1.0 nm) short-period superlattice (sample 2).

(b) Schematic potential diagram of the GaAs/ $\text{Al}_{0.17}\text{Ga}_{0.83}\text{As}$  triple QW structure. Nominal well widths are 7.8 nm (QW1), 5.5 nm (QW2), and 3.5 nm (QW3). The calculated energies of the interband transitions between the first confined electron and hole states at low temperatures are listed and indicated by vertical arrows.

and 280 K in a closed-cycle He cryostat using a cw He-Ne laser at 632.8 nm for excitation and a conventional lock-in technique for detection. Time-resolved PL spectra were measured between 30 and 280 K also in a closed-cycle cryostat using a laser diode with 52-ps pulses at 653 nm for excitation and a streak-scope system for detection. The time resolution of this system is about 200 ps.

### 3. Results and discussion

Figures 2(a) and 2(b) show the steady-state PL spectra of samples 1 and 2, respectively, measured for  $T$  between 20 and 240 K. For each spectrum, the PL intensity is normalized to its maximum value. At 20 K, the PL spectra of both samples consist of three emission bands originating from QW1 (1.56 eV), QW2 (1.59 eV), and QW3 (1.63 eV). The split structures are observed for QW2 and QW3 due to the formation of growth islands [4], which indicates the high quality of our samples. When  $T$  is increased, the PL peaks shift to the lower energy side according to the empirical relation by Varshni  $E(T)=E(0)-\alpha T^2/(\beta+T)$ , where  $E(0)$  denotes the transition energy at 0 K.  $\alpha$  and  $\beta$  are the Varshni thermal coefficients, whose values agree with those found in the literature for GaAs [5].

It is important to note that the PL spectra of sample 1 show a non-uniform intensity distribution, in particular at low temperatures. The PL intensity for QW1 is

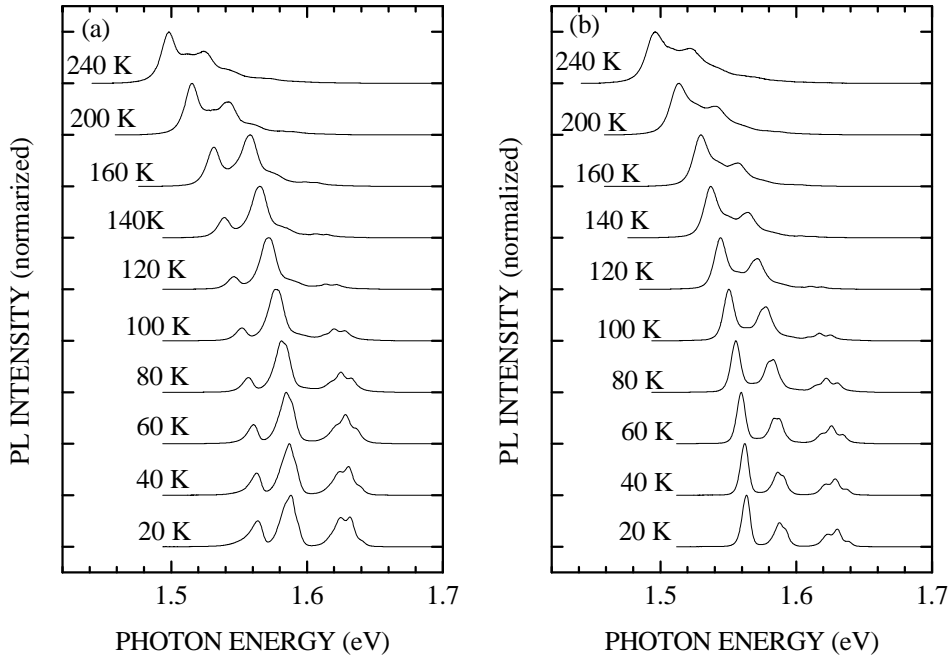


Fig. 2 Temperature dependence of the cw PL spectra of (a) sample 1 and (b) sample 2. The PL intensities are normalized to the maximum peak intensity in each spectrum. The base lines of the PL spectra are shifted for clarity.

much weaker than the one for the other wells. However, the dominant signal of QW1 above 200 K implies that the photoexcited carriers, which are initially in the non-equilibrium state, are much more efficiently scattered by phonons so that they are thermalized before radiative recombination can occur. The PL peak intensity thus monotonously decreases above 200 K as the emission photon energy increases, reflecting a thermal population. Therefore, the PL intensity distributions at high temperatures can easily be understood in terms of thermalized and partially ionized excitonic emissions [6]. However, in sample 2, the PL intensity distribution at low temperatures shows the typical one with the highest PL intensity for the widest QW. At higher temperatures, the PL intensity also monotonously decreases as the emission photon energy increases, reflecting the thermal population. A striking feature we found for sample 1 is that the PL intensity distribution among the three wells strongly depends on  $T$ , especially at low temperatures.

In order to obtain more information on the PL properties, in particular with regard to the carrier dynamics, we recorded time-resolved PL spectra for different temperatures. Figures 3(a) and 3(b) show time-resolved PL traces for each QW in

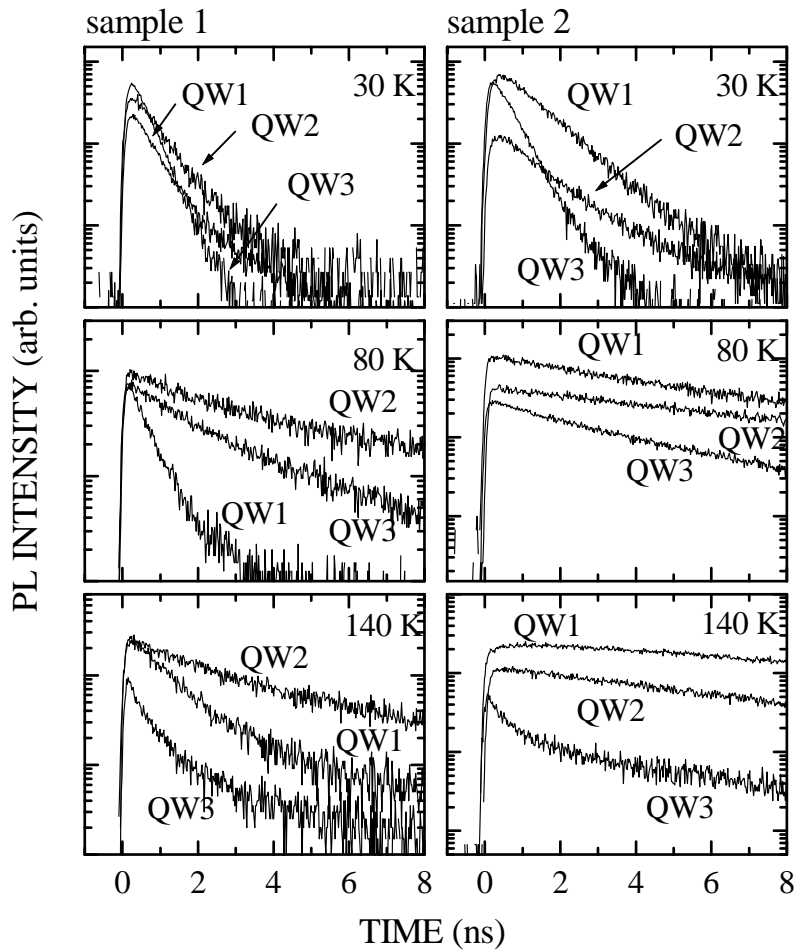


Fig. 3 PL transients of QW1, QW2, and QW3 in sample 1 (left) and sample 2 (right) recorded at 30, 80, and 140 K plotted on a semi-logarithmic intensity scale.

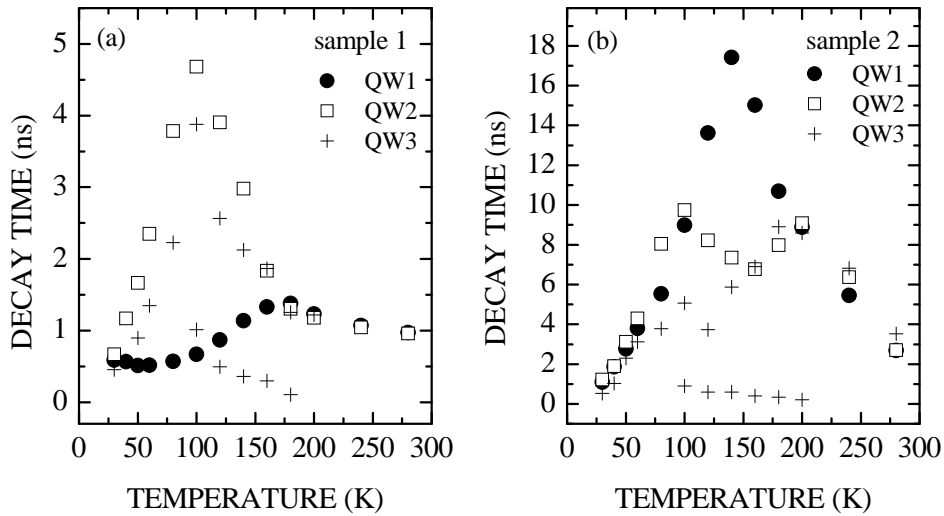


Fig. 4 Temperature dependence of the PL decay time for each QW in (a) sample 1 and (b) sample 2. The PL transients for QW3 above 100 K consist of biexponential decays with two time constants.

sample 1 and 2, respectively, recorded at 30, 80, and 140 K. The temperature dependences of the respective PL decay times are shown in Fig. 4.

In sample 1, the PL transients for each QW show nearly single-exponential decays at 30 K, whose decay times are 0.6, 0.7, and 0.5 ns for QW1, QW2, and QW3, respectively. These values appear to be mainly determined by the radiative recombination lifetime. When  $T$  increases up to 80 K, the decay time of QW1 hardly changes, while for QW2 and QW3 they increase up to 3.8 ns and 2.2 ns, respectively. This behaviour observed for QW2 and QW3 can be understood by considering the increased lifetime of the radiative recombination with increasing  $T$  [7]. However, the temperature behaviour observed for QW1 cannot be explained by the same argument. When  $T$  increases up to 140 K, the decay time of QW1 increases up to 1.2 ns in sample 1. This observation suggests that the anomalous temperature evolution of the PL decay time at low temperatures cannot be ascribed to an enhancement of non-radiative recombination channels for the first QW grown after the alloy cladding layer [8]. Therefore, the anomalous temperature dependence of the decay time observed for QW1 at lower temperatures reflects the particular emission processes in this composite QW system, which we ascribe to the competition between carrier relaxation and capture dynamics. With a further increase of  $T$  up to 200 K, the PL decay times become very similar for all three QWs due to the thermalization.

In sample 2, the usual temperature dependence of the PL lifetime is observed as shown in Fig. 4. At 30 K, the PL decay times are found to be 1.1, 1.2, and 0.5 ns for QW1, QW2, and QW3, respectively. They increase to 5.5 (QW1), 8.0 (QW2), and 3.8 ns (QW3) with increasing  $T$  up to 80 K due to the increased lifetime of radiative recombination. Above 100 K, the PL transients exhibit a non-exponential decay curve for QW3 and a slow increase before the decay for QW1 and QW2 as shown in Fig. 3 for

sample 2 at 140 K. This observation indicates the detrapping and transfer process: photoexcited carriers in QW3 are scattered by phonons and captured by other wells, before radiative recombination can occur, so that they are transferred to QW1 and QW2. When  $T$  increases to 200 K, the PL decay times are nearly the same for all three QWs, because the carriers in all QWs are thermalized.

We may consider the following reasons why the cladding layers should be responsible for the different behaviours. Due to the different cladding layers, the potential distribution of the subband edges might be different between the two samples, so that the second subband in the widest well might be in one sample above and in the other sample below the barrier. These variations of the relative energy positions of the excited states might influence the luminescence dynamics because of the different outer confinement effects. Since the QWs and barriers in both samples are nominally undoped with a typical p-type residual density of a few  $10^{14} \text{ cm}^{-3}$ , any effects due to internal electric fields can be neglected. However, to identify the origin of the different PL properties for the two cladding layer configurations, further detailed experimental and theoretical analyses are necessary.

#### 4. Conclusion

The effect of different cladding layer configurations on the PL properties has been studied for GaAs triple QWs embedded in  $\text{Al}_{0.17}\text{Ga}_{0.83}\text{As}$  barriers using steady-state and time-resolved PL experiments as a function of lattice temperature. An anomalous temperature dependence of the PL properties for the widest QW (QW1) is observed in the sample with  $\text{Al}_{0.3}\text{Ga}_{0.7}\text{As}$  ternary alloy cladding layers (sample 1). The PL intensity at low temperatures is much weaker for QW1 than for the other QWs. Furthermore, the PL transients of QW1 hardly change with respect to the decay time with increasing  $T$ , which differs from the temperature dependence expected for the excitonic radiative recombination lifetime. However, the sample with GaAs/AlAs short-period superlattice cladding layer (sample 2) exhibits the usual temperature dependence for the PL intensity and decay time. The anomalous temperature dependence of the PL properties observed in sample 1 at low temperatures is a result of a competition between carrier relaxation and capture processes of photoexcited carriers.

#### References

- [1] Tomita A, Shah J, and Knox R S 1996 Phys. Rev. B 53 10793-803
- [2] Kim D S, Ko H S, Kim Y M, Rhee S J, Hohng S C, Yee Y H, Kim W S, and Woo J C 1996 Phys. Rev. B 54 14580-8
- [3] Schrottke L, Grahn H T, and Fujiwara K 1997 Phys. Rev. B 56 13321-5
- [4] Fujiwara K, Jahn U, Hey R, Kastrup J, and Grahn H T 1995 J. Cryst. Growth 150 43-8
- [5] Casey H C and Panish M B 1978 Heterostructure Lasers (New York Academic)
- [6] Fujiwara K, Tsukada N, and Nakayama T 1988 Appl. Phys. Lett. 53 675-7
- [7] Feldmann J, Peter G, Göbel E O, Dawson P, Moore K, and Foxon C 1987 Phys. Rev. B35 8281-4
- [8] Petroff P M, Miller R C, Gossard A C, and Wiegmann W 1984 Appl. Phys. Lett. 44 217-9